STOCHASTIC RESONANCE IN THE NONAUTONOMOUS CHUA'S CIRCUIT

by

V. S. Anishchenko, M. A. Safonova, and L. O. Chua

Memorandum No. UCB/ERL M92/51

15 May 1992

STOCHASTIC RESONANCE IN THE NONAUTONOMOUS CHUA'S CIRCUIT

by

V. S. Anishchenko, M. A. Safonova, and L. O. Chua

Memorandum No. UCB/ERL M92/51

15 May 1992

ELECTRONICS RESEARCH LABORATORY

College of Engineering
University of California, Berkeley
94720

TITLE PAGE

STOCHASTIC RESONANCE IN THE NONAUTONOMOUS CHUA'S CIRCUIT

by

V. S. Anishchenko, M. A. Safonova, and L. O. Chua

Memorandum No. UCB/ERL M92/51

15 May 1992

ELECTRONICS RESEARCH LABORATORY

College of Engineering
University of California, Berkeley
94720

STOCHASTIC RESONANCE IN THE NONAUTONOMOUS CHUA'S CIRCUIT

V.S.Anishchenko, M.A.Safonova

Physics department
Saratov State University
Saratov, Russia

L.O.Chua

Electronics Research Laboratory
University of California, Berkeley

Abstract

The dynamics of the nonautonomous Chua's circuit driven by a sinusoidal signal and additive noise is investigated numerically via the "two-state" dynamics method. The possibility to realize the phenomenon of stochastic resonance (SR) is established. The SR is characterized by an increase in the signal-to-noise ratio (SNR) due to the coherent interaction between the characteristic frequencies of the chaotic bistable Chua's circuit and the modulation frequency of the input. The SNR can be controlled by both external noise and system parameter variations in this circuit. The statistical characteristics of the "chaos-chaos" type intermittency and their correlation with the optimal conditions for SR are investigated.

This work is supported in part by the Office of Naval Research under grant N00014-89-J-1402 and the National Science Foundation under grant MIP-8912639.

1. Introduction

The phenomenon of stochastic resonance (SR) is observed in bistable nonlinear systems driven simultaneously by external noise and a sinusoidal force. In this case, the signal-to-noise ratio (SNR) increases until it reaches a maximum at some noise intensity D. This optimum noise intensity D depends on the bistable system and the frequency of the external sinusoidal force[1-7].

The mechanism of the SR-phenomenon is as follows. In the absence of a periodic modulation signal the noise alone results in a random transition between the two states of the bistable system. This random process can be characterized by the probability density $p(t)$ of the residence times of the system at one of the states and, therefore, by some mean switching frequency ω_s. This mean switching frequency depends on the noise intensity D and the height of the potential barrier separating the two system states[1-13].

In the presence of an external modulation imposed by the sinusoidal signal signal $\varepsilon_0 \sin \omega_0 t$, the potential barrier changes periodically with time. The modulation signal amplitude ε_0 is assumed to be sufficiently small so that the input signal alone does not induce transitions in the absence of noise. A coherence phenomenon between the modulation frequency ω_0 and the mean switching frequency ω_s emerges when the system is simultaneously driven by a periodic signal and a noise source. As a result, a part of the noise energy is transformed into the energy of the periodic modulation signal so that the SNR increases. This phenomenon is qualitatively similar to the classical resonance phenomenon. However, unlike in classical circuit theory where one "tunes" the input frequency ω_0 to achieve resonance in an RLC circuit, here ω_0 is fixed at some arbitrary convenient value and

one "tunes" the noise intensity D to achieve stochastic resonance. Since the switching frequency ω_s is the statistical mean value of the random process of transitions in the bistable system, it is natural, to call the above phenomenon a stochastic resonance.

The SR-phenomenon can be realized not only in bistable systems, but it can also take place in multistable systems, as well as in systems forced by an arbitrary (non-sinusoidal) periodic signal. However, in such cases, it is necessary to use a noise perturbation to induce a random switching process into the system in order to realize the SR phenomena.

In this paper we will generalize the above classical to SR phenomenon to a broader class of dynamical systems. For this purpose, let us consider the class of quasi-hyperbolic systems[14]. Many regular (fixed points, limit cycles,torus) and chaotic attractors can coexist simultaneously in the state space of such systems. These attractors can interact with each other[15-19]. The classical example of such interaction is an intermittency of the "cycle-chaos" type[14]. In this paper, we consider a more general case of attractor interactions, henceforth called a "chaos-chaos" type intermittency[20-23].

Two chaotic attractors separated in state space by a separatrix hypersurface can merge into one chaotic attractor. The phenomenon of this "chaos-chaos" type intermittency is observed in a small range of some control parameter μ greater than some critical parameter value μ^* where the merging of the attractors takes place. Since the statistical properties of this kind of intermittency is identical to that observed from classical bistable systems, it can be considered as a generalized form of bistable behavior in chaotic dynamical systems. If the control parameter value $\mu<\mu^*$, the transition can be induced by the noise source. In this case, the statistical characteristics of the intermittency phenomenon will depend on the noise

intensity D. If $\mu>\mu^*$, the transition process is caused only by the properties of the dynamical system.

In general, quasi-hyperbolic systems which exhibit the above intermittency phenomenon must have two co-existing chaotic attractors. The mean frequency of the random process of transitions in such systems can be controlled by both system parameters (in the absence of noise) and external noise (when the parameters are fixed).

The phenomenon of SR can be observed in systems which exhibit a "chaos-chaos" type intermittency phenomenon when driven by a periodic modulation signal. This was first demonstrated in Ref.24 for the one-dimensional cubic map and for the classical Lorenz system with parameter values chosen in the quasi-attractor region ($r>>1$). In this paper we investigate the possibility for realizing the SR-phenomenon and examine its properties in Chua's circuit[25].

2. Driven Chua's circuit

We shall investigate the phenomenon of the stochastic resonance in the following system:

$$\begin{aligned} \frac{dx}{dt} &= \alpha(y - h(x)) \\ \frac{dy}{dt} &= x - y + z \\ \frac{dz}{dt} &= -\beta y + \varepsilon_0 \sin \omega_0 t + \xi(t), \end{aligned} \tag{1}$$

where

$$h(x) = m_1 x + \frac{1}{2}(m_0 - m_1)(|x+1| - |x-1|),$$
$$<\xi(t)> = 0, \quad <\xi(t)\xi(t+\tau)> = D\delta(\tau) \tag{2}$$

when $<\cdot>$ and $\delta(\cdot)$ denote the averaging operator and the delta function, respectively.

The noise source $\xi(t)$ and the sinusoidal input with amplitude ε_0 and frequency ω_0 are inserted in the third equation because they correspond to the more practical way of inserting voltage sources in the laboratory to the physical circuit, thereby simplifying our future comparison with the numerical simulation results to be reported in this paper.

We fix the parameter values $m_0 = -1/7$, $m_1 = 2/7$ (as in Ref[25]) so that only the values of α and β will be changed. The 2-parameter bifurcation diagram for system (1) (with $D=0$ and $\varepsilon_0=0$) is shown in Fig.1[25]. A limit cycle Γ_1 (and the its symmetrical image Γ_{-1}) are spawned abruptly on the curve 1. Then they undergo a sequence of period-doubling bifurcations. This process led to the birth of a pair of symmetrical Rossler-type attractors. They exist, separated from each other, in the region bounded by curves 1 and 2 of the bifurcation diagram in Fig.1. The bifurcation curve 2 corresponds to the birth of a double scroll attractor (DSA). The DSA, which results from the merging of two symmetrical Rossler-type attractors, exists in the shaded region in Fig.1 bounded between curves 2 and 3.

The system (1) can be interpreted as a bistable nonlinear oscillator with two symmetrical chaotic attractors in the region bounded between curves 1 and 2. Since the basins of these attractors are separated by a two-dimensional invariant manifold (separatrix surface) they can not intersect each other. Any interaction between these two attractors can be induced only by external perturbations.

When the two attractors of the autonomous system merge on the curve 2 the

separatrix surface is destroyed, thereby giving rize to the phenomenon of a dynamical "chaos-chaos" type intermittency. This phenomenon corresponds to the emergence of the DSA due to the interaction of the two attractors of the autonomous system. Consider next the region bounded by curves 2 and 3 but in the vicinity of curve 2. In this case, the phase trajectory resides in each attractor for a long time and makes relatively few transitions between them. The switching frequency ω_s is very small here ($\omega_s << 1$). If we move further to the right from curve 2, hovewer, the switching frequency increases.

Hence, the system 1 is a quasi-hyperbolic system which exhibits a bistable regime of chaotic oscillations. The interaction between these chaotic attractors which led to a "chaos-chaos" type intermittency phenomenon can be induced by either adding a noise source, or by varying the parameter α or β. Therefore, the system (1) is a very convenient vehicle for exploring the SR phenomenon in chaotic systems.

3. Methods of analysis

To investigate the SR-phenomenon it is necessary to compute some important time series characteristics. We will pause therefore to enumerate these characteristics and comment on the methods we used to calculate them in this paper.

3.1. Calculation of the residence time probability density $p(\tau)$ for the individual attractor: method of "two-states" dynamics.

There are two methods for analyzing the behavior of bistable systems: the complete dynamics method and the "two-state" dynamics method. In first case one of

the variable of the system, for example, $x(t)$, is considered as the output signal, without any further processing. In the second case, an additional filtering operation is made on the signal $x(t)$, where it is replaced by a "telegraph" signal $w(t)$, which at any time t is equal to +1 or -1 if the trajectory resides in one or the other attractor, respectively. In this case, we lose the information on the dynamical behavior of the system inside each of the attractors. Instead we can obtain a more precise characterization of the transition process.

As we already know, two independent symmetrical strange attractors co-exist in the region bounded by curves 1 and 2 of the bifurcation diagram in Fig.1. Transitions between them can take place by either applying a noise perturbation, or by varying the parameter α or β into the region bounded by bifurcation curves 2 and 3. To calculate the output corresponding to the "two-state" dynamics, it is only necessary to determine on which of the attractors is the trajectory evolving at any given moment of time during the entire numerical integration process. Projection of both attractors onto the x-y plane and the y-z plane are shown in Fig.2. It is generally difficalt to derive the equation of the surface separating these attractors in the state space. In this paper, we will use the following algorithm to identify the moment of transition approximately: during each step of our numerical integration computation we check the condition:

$$(|x(t_i)| - 1)(|x(t_{i-1}| - 1) < 0, \tag{3}$$

where $t_i=i\Delta t$, Δt is the step size of integration, $i = 0,1,...,I$, $I\Delta t=t_{max}$, t_{max} is the final time of integration. Observe that condition (3) implies an intersection between the trajectory and one of planes $x=\pm 1$ at $t_{i-1}\le t\le t_i$. The times t_k^*, $k=1,2,...,K$, corresponding to these intersections are stored. If the inequality

$$r_k = x(t_k^*)x(t_{k+1}^*) > 0, \tag{4}$$

holds, then the trajectory did not leave the attractor at t_{k+1}^* (it has crossed the same plane twice one after the other). If $r_{k_1}<0$ for some k_1, than the trajectory has crossed two different planes successively and, therefore, a transition takes place within the interval $(t_{k_1}^*, t_{k_1+1}^*)$. This algorithm is related to the geometry of the equilibrium points locations and their eigenspaces in the phase space of the system (1)[25]. In this case, the moment of transition is calculated as the average of the times corresponding to two successive intersections of different planes:

$$t_l^{**} = (t_{k_1+1}^* - t_{k_1}^*)/2, \quad l=1,2,...,L, \tag{5}$$

and the residence time t_l of the trajectory inside one of the attractors is determined by the difference between two successive transition time:

$$t_l = t_{l+1}^{**} - t_l^{**}, \quad l=1,2,...,L. \tag{6}$$

Correspondingly, the output $w(t)$ changes its value from +1 to -1, or vice-versa, at the moment t_l^{**}. Fig.3 illustrates the typical behavior of the waveform $x(t)$ and its associated "pulse-width modulated" square wave $w(t)$ for the case where the transitions are induced by noise (Fig.3,a,b), and by varying the parameter α (Fig.3,c,d).

Without loss of generality, the residence times probability density $p(t)$ needs to be calculated at only one of the attractors. Hence, we determine only the time intervals t_l corresponding to the transition from $w(t_l^{**})=+1$ to $w(t_{l+1}^{**})=-1$. Then an estimate of the probability density is calculated over this sample as a histogram of

normalized values of t_l relative to some partition $\tilde{\Delta}t$:

$$p(t_m) = L_m/L, \tag{7}$$

where $t_m = m\tilde{\Delta}t$, $m=1,2,...,M$, $M=\tilde{t}_{max}/\tilde{\Delta}t$, $\tilde{t}_{max}$ denotes some fixed maximal value of the residence time, and L_m denotes the number of $t_l \in (t_{m-1},t_m)$. We have chosen $\tilde{t}_{max} \cong 300$, $t_{max} \in (2*10^5, 4*10^5)$, $\Delta t=0.1$, $\tilde{\Delta}t=0.5$.

The mean residence time for the trajectory to remain in the vicinity of each attractor can be determined from the probability density $p(t)$; namely,

$$T_s = \langle t \rangle \overset{\Delta}{=} \int_0^\infty tp(t)dt \tag{8}$$

Hence, we can define the mean switching frequency by

$$\omega_s = 2\pi/T_s \tag{9}$$

In numerical calculations the integral in (8) is of course replaced by an approximate discrete sum:

$$T_s = \langle t \rangle = \tilde{\Delta}t \sum_{l=1}^{L} t_l p(t_l). \tag{10}$$

3.2. Calculation of the power spectrum: determination of the SNR

Let us define the signal-to-noise ratio (SNR) by the relationship:

$$\mathrm{SNR} = 10 \ln \frac{S_N(\omega_0)+S_M(\omega_0)}{S_N(\omega_0)}, \tag{11}$$

where $S(\omega)$ is the power spectrum density of $x(t)$ or $w(t)$, $S_N(\omega_0)$ is the power spectrum density of the noise background at the frequency ω_0, and $[S_N(\omega_0)+S_M(\omega_0)]$ is superimposed power spectrum density of the modulation signal and the noise background at the same frequency. Hence, the value of SNR can be calculated from the computed data from of the power spectrum $S(\omega)$ in the presence of the modulation signal. All SNR calculations in this paper are based on (11).

Let Λ_D, Λ_α, and Λ_β denote the relationship between the signal-to-noise ratio (SNR) and the noise intensity D, the parameter α, or the parameter β, respectively where $D\in[D_1,D_2]$, $\alpha\in[\alpha_1,\alpha_2]$, and $\beta\in[\beta_1,\beta_2]$. The presence of an extremum point (maximum) in Λ_D, Λ_α, or Λ_β for some $D^*\in[D_1,D_2]$, $\alpha^*\in[\alpha_1,\alpha_2]$, or $\beta^*\in[\beta_1,\beta_2]$ is our main evidence of the presence of stochastic resonance phenomenon. In other words, a "bell-shape" curve for Λ_D, Λ_α, or Λ_β indicates the existence of SR.

The power spectrum is computed by the standard fast Fourier transform (FFT) algorithm. The FFT is first calculated many times for different samples of the output signal $x(t)$ or $w(t)$ with a modest sample length $t_2-t_1\cong 410$. The above computed FFT data is averaged to obtain the final power spectrum. In our simulation the number of data used in the averaging ranges from 100 to 1000. To increase the precision of our power spectrum we use the window:

$$S^*(\omega_i) = 0.54S(\omega_i) + 0.23(S(\omega_{i-1}) + S(\omega_{i+1})). \tag{12}$$

Fig.4 represents the results obtained by using the algorithm for computing the power spectrum of $x(t)$ at α=8.9, β=14.286, ε_0=0.1, f_0=0.6, D=0. The of number data used in our averaging is 300. Two spectra are shown. The first one was calculated for the raw signal $x(t)$ (the complete dynamics method) and has, in addition to the sharp peak at the frequency ω_0, a smooth local maxima in the frequency neigborhood related to the characteristic time of the Rossler type attractor (Fig.4,a). The second power spectrum was calculated from the processed "telegraph" signal $w(t)$ (the "two-state" dynamics method) (Fig.4b). In this case, the peak at same frequency ω_0 remains, but the information concerning the internal behavior (e.g., the local maxima in $x(t)$) on each of the attractors is lost.

4."Chaos-chaos" type intermittency: statistical analysis of the switching process.

Consider the point α=8.6, β=14.286 near the bifurcation curve 2 in the region of existence of two symmetrical Rossler type attractors (see the diagram in Fig.1). Let us induce the intermittency phenomenon with the help of the noise source in (1). Then, integrating the system for a long time and using the "two-state" dynamics, we shall calculate the probability density of the residence time of the trajectory in one of the attractors in the absence of the an external sinusoidal modulation (ε_0=0). Figure 5 shows the typical results of our computations of the probability density $p(\tau)$ (here τ is the normalized time, i.e. $\tau=t/T_0$, $T_0=2\pi/\omega_0$), the power spectra $S_w(\omega)$ corresponding to the telegraph signal $w(t)$, and the one-dimensional probability density $p(x)$ (the latter is calculated by the complete dynamics method). Let us move on the α-β parameter plane to the region of existence of the DSA (α=8.9, β=14.286) in

the vicinity of the bifurcation curve 2 and perform the same computation without noise (D=0). The results are shown in Fig.6. A comparison between Fig.5 and Fig.6 shows that there are two mechanisms for inducing the the "chaos-chaos" type intermittency in system (1): a strictly dynamical mechanism (Fig.6) and a noise-induced mechanism (Fig.5). Observe that the statistical characteristics of the two intermittent waveforms are qualitatively similar in both cases.

Let us examine an interesting peculiarity in the above probability density distributions $p(\tau)$: in both Figs.5 and 6, the successive relatively sharp maxima of the function $p(\tau)$ occurs at discrete multiples of a basic time interval $\Delta\tau \approx 0.22$. This means that on the average, transitions from one attractor to the other can occur only at discrete moments of time $n\Delta\tau$ (n=1,2,3,...). In the case of the noise-induced intermittency, the envelope of $p(\tau)$ decreases approximately in accordance to an exponential law as function of τ (Fig.5). In the case of the dynamical intermittency, two peaks corresponing to n=5 and n=9 stand out above the background an other wise exponentially decreasing envelope which passes approximately through the series of extremum points (maxima) of $p(\tau)$ (Fig.6). This means that the probabilities of transitions at n=5 and n=9 are significantly higher than the probabilities at the other values of n. The above phenomenon of the discretization of the probability density function $p(\tau)$ in system (1) is extremely interesting and warrants a more detailed analysis.

The discretization of the probability density function $p(\tau)$ with a time step size equal to $\Delta\tau$ means that the system (1) has the same characteristic time constant in its dynamics. It is natural to conjecture that this basic time constant is connected with the fundamental period of the dominant but unstable limit cycle which is contained in the closure of the Rossler type attractor, spawned via a sequence of period-doubling bifurcations. Our computation confirms this. Figure 7 shows the phase

portrait and the power spectrum of the Rossler type attractor in the system (1) at α=8.6, β=14.286. The basic frequency $\omega_R=2\pi/T_R\approx 2.8$ ($T_R\approx 2.31$, $\tau_R=T_R/T_0\approx 0.21$) corresponding to the highest peak is identified in the power spectrum. The same characteristic time constant $\Delta\tau\approx\tau_R$ is found to apply also in the DSA-regime in the vicinity of the bifurcation curve 2, as shown in Fig.8.

The regular discrete structure of $p(\tau)$ in Fig.5 and Fig.6 can now be explained. The phase trajectory of the system (1) makes a transition after making certain integer number of rotations around one of the equilibrium points $P^{\pm}$. The duration of each rotation corresponds approximately to τ_R. Therefore, transitions can only occur approximately at the discrete times $\tau_s\cong n\tau_R$, n=1,2,3.... The results of our calculation in Fig.5 and Fig.6 confirm this transition mechanism.

Let us investigate next the structure of the probability density function $p(\tau)$ in the presence of an external sinusoidal perturbation to the system (1) ($\varepsilon_0\neq 0$). Our statistical analysis was conducted for 3 cases: the noise-induced intermittency case, the strictly dynamical case (in the DSA-regime), and the combined case of DSA-regime in the presence of noise. The results are found to be qualitatively equivalent for all three cases.

Figure 9 shows the typical probability density $p(x)$ and the associated power spectrum $S(\omega)$ in the presence of a small sinusoidal excitation having an amplitude ε_0=0.1 and frequency ω_0=0.6 in the absence of noise D=0.

The symmetrical distribution $p(x)$ about x=0 implies equal probabilities for the phase trajectory to reside in the vicinity of each equilibrium point (P^+ or P^-). The power spectrum has a noise background similar to that associated with the intermittency phenomenon and a sharp peak located at the modulation frequency ω_0 [11,12].

The second characteristic time constant of the system is due to the modulation

frequency. Since the system's potential barrier is changed periodically in this case, the structure of the residence time probability density function $p(\tau)$ must change in such a way as to manifest the presence of two characteristic system time constants T_R and T_0 in this case!

Figure 10 shows the results of our calculation of $p(\tau)$ for three different values of the modulation frequency: ω_0=0.4, 0.6 and 0.8. The structure of $p(\tau)$ has undergone an obvious modification. Namely, the maxima of $p(\tau)$ are concentrated near the discrete times $m/2$ (m=1,3,5,...). At ω_0=0.4, observe that the set of maxima of $p(\tau)$ decreases exponentially as a function of m=1,3,5,.... For ω_0=0.6 and 0.8, the exponential decay is observed at $m\geq 3$. The finer structure of $p(\tau)$ can be seen in the neighborhood of each maxima located near $\tau=m/2$, m=1,3,5,.... Thus, the probability density function $p(\tau)$ contains the information concerning the presence of two characteristic system time constants T_R and T_0.

When the system (1) is operating in a chaos-chaos type intermittency regime, it exhibits a third characteristic time constant; namely: the mean switching time T_s. This time constant determines the mean switching frequency ω_s (see Eq.(9)), depending on the noise intensity D, and on the system parameters α and β. The results of our computation of these dependencies in the presence of an external modulation signal are shown in Fig.11. Observe that the mean switching frequency ω_s increases nearly linearly with respect to an increase of the noise intensity, and an increase in the distance from the curve 2 within the DSA-region in the α-β plane. The results of Fig.11 demonstrates in a convincing way the possibility to control the switching frequency by varying the noise intensity D or the values of the parameters α and β in the systems (1). Hence, we can control the third characteristic time constant $T_s=2\pi/\omega_s$ in system (1).

The structure of the probability distribution functions $p(\tau)$ in Fig.10 can be

explained by the coherent interaction between the external modulation frequency ω_0 and the mean switching frequency ω_s. In the case of the classical SR phenomenon, the typical structures of $p(\tau)$ is similar to those of Fig.10. Such a structure is typically associated with an increase of the SNR[10-12]. Thus, the data of Fig.10 and Fig.11 predict the possibility to realize the SR-phenomenon in Chua's circuit.

5. Numerical simulation of stochastic resonance phenomenon

Let us choose the point α=8.6, β=14.286 in the Rossler attractor region of the α-β parameter plane in Fig.1 as an initial point of the system (1) and investigate the possibility of the realization of the SR-phenomenon. Let us move the parameter α value to the right into the DSA-region. The values of the amplitude and the frequency of the sinusoidal modulation input are fixed at ε_0=0.10 and ω_0=0.6, respectively. The dependencies of the signal-to-noise ratio on α for different values of the noise intensity D are shown in Fig.12. These plots demonstrate the SR-phenomenon. The maximum value of the SNR reaches the value $\cong$ 21 at α=8.8 in the absence of noise. The noise perturbation (with constant intensity $D\neq0$) does not have a significant influence on the SR phenomenon except for a small decrease of the SR value. For example, the maximum value of the of SNR decreases to 19.5 when $D=10^{-3}$, and to 16.4 when $D=10^{-2}$. The mean switching frequencies ω_s are values related to the maxima of the SNR, and are very close to each other in all three cases in Fig.12, we have 0.258 (D=0), 0.245 ($D=10^{-3}$) and 0.243 ($D=10^{-2}$).

The residence time probability density functions $p(\tau)$ shown earlier in Fig.10(b) also behaves in the same way for values of α corresponding to the maxima of SNR (see Fig.10). In other words, the behavior of the function $p(\tau)$ is not changed qualitatively in the presence of noise, as verified by the results shown in Fig.13.

An absolutely analogous behavior is observed when the parameter β is changed (with α=8.6). The plot of the dependency of SNR(β) is shown in Fig.14 for D=0. The addition of noise results in a change in the SNR(β), which is qualitatively equivalent to Fig.12. Observe that the critical value β=13.886 in Fig.14, which corresponds to the maximum value of the SNR ($\approx$21.4), is related to the mean switching frequency ω_s=0.248!

Let us investigate next the SR phenomenon as a function of the noise intensity D. For this purpose we shall choose the parameter value α=8.6<α_{cr} so that the two symmetric Rossler attractors have not yet merged. Inducing transitions by adding a noise source of intensity D, we obtain the dependence of SNR(D), which is shown in Fig.15. The effect of SR is deducted in this case. The SNR is equal 11.5 at D=0.01, which is obviously less than those in Fig.12(c). The values of the mean switching frequency ω_s are also different from the previous results: $\omega_s \in (0.11,0.13)$ at $D \cong 0.01$.

We can give a physical explanation for the above observations. The potential barrier of the bistable system changes with the modulation frequency ω_0 in the presence of an external sinusoidal excitation. State transitions take place at a mean switching frequency which is related to the mean residence time in one of the attractors. Since the intermittent trajectory must traverse around 2 attractors, it follows that the condition of the resonance is given by $\omega_s=2\omega_0$. The other words, the double mean residence time $2T_s$ is equal to the period T_0 of the external force. This situation corresponds to the condition of coherence between the switching process and the modulation. The resonance condition $2\omega_0=\omega_s$ is optimal, but not unique.

As seen from Fig.10 and Fig.13, the residence time τ corresponding to SR are centered near the values $\tau=m/2$, m=1,3,5,7,.... This means that the switching process is characterized by a discrete sequence of mean switching frequencies ω_s^m. The condition $\omega_s^1=2\omega_0$ (m=1) gives the frequency corresponding to the dominant peak.

Resonances at subharmonic frequencies $\omega_S^3=2\omega_0/3$ (m=3), $\omega_s^5=2\omega_0/5$ (m=5) etc. can take place as well.

The above reasoning explains the results presented in Figs.12, 14 and 15 completely. Indeed, the maximum SNR occurs at values of $\omega_s \in (0.24,0.25)$ under variation of the parameters α and β, both in the presence of noise, and without noise (D=0). These values of ω_s are close to the case m=5 because $\omega_s^5=2\omega_0/5$ is equal to 0.24 for ω_0=0.6. If the noise intensity increases, than the mean switching frequency decreases significantly. The maximum SNR in Fig.15 is related to the value ω_s=0.13. It is not difficult to verify that the weak resonance m=11 which corresponds to $\omega_s=2\omega_0/11$=0.111 also takes place.

By changing the amplitude, frequency of modulation, or system parameters, we can derive the conditions for realizing the basic resonance $\omega_s=2\omega_0$. Figures 16 and 17 show the results obtained at ω_0=0.35 and ε_0=0.15. Variation of the modulation parameters ε_0 and ω_o will result in a reshaping of the structure of the distribution function $p(\tau)$. The maximum values of $p(\tau)$ has shifted to the vicinity of τ=1/2. Simultaneously, the transitions probability related to the condition of the basic resonance $\omega_s=2\omega_0$ has increased strongly. The SR-phenomenon takes place both in the absence of noise (Fig.16), and in the presence of noise having an intencity D within the range $10^{-4} \le D \le 10^{-1}$ (Fig.17, $D=5*10^{-3}$). The plot of the SNR versus the noise intensity D is shown in Fig.18. This plot demonstrates the SR-phenomenon at fixed values of system parameters.

The above results verified our earlier conclusion in Section 4 concerning the possibility for attaining stochastic resonance in Chua's circuit. Observe that the results shown in Figs.12-18 actually reflect the coherent interaction process between only two characteristic system time constants (respectively, natural frequencies); namely: T_0 and T_s (respectively ω_0 and ω_s). Recall, however, that the system (1) has

a third characteristic time constant T_R which reflect the complicated system dynamics inside each of the interacting attractors. Additional conditions can be derived to relate the SR-phenomenon to the characteristic system time constant T_R.

Let us examine next the results shown in Fig.19 when D=0. Observe that there are two values (α=4.1 and α=4.26) of the parameter α where the SNR is close to 41.5! What mechanism is responsible for such an unusually strong increase in the SNR? For these values of α the double scroll attractor is observed without external modulation (ε_0=0). Interestingly enough, the double scroll attractor is suppressed and replaced by a complicated limit cycle when driven by a sinusoidal signal with ε_0=0.07 and ω_0=0.25 in the nonautonomous system (1). The period of this stable limit cycle is exactly equal to the period of the modulation signal; namely, $T_0 \cong 25$! In this case, the double mean switching frequency is a deterministic variable whose value is exactly equal to the modulation frequency $2\omega_s=\omega_0=0.25$. This limit cycle, and its power spectrum, are shown in Fig.19,(b) and (c), respectively.

Thus, at D=0, the classical resonance phenomenon is observed when the frequency of the periodic force is equal to the frequency of the limit cycle. The amplitude of the modulation signal is greatly amplified here in view of the phase-locking phenomenon.

Figure 20 shows the influence of noise under this classical resonance regime. Observe that as the noise intensity increases, the regularity of the switching process is destroyed and the classical resonance regime changes into a stochastic resonance regime.

The increase in the SNR during stochastic resonance can be interpreted as a process of redistribution of energy through an optimal choice of control parameters of the system (1). This swapping of energy is clearly seen in the calculated power spectrum shown in Fig.21. Observe that in the absence of a modulation signal, the

power spectrum (dashed curve) is located above the curve $S(\omega)$ (calculated in the the presence of the modulation) at all frequencies except near the resonance frequency ω_0. The total energy in each case is equal to the area under the curve and is found to be constant. Therefore, the energy of the modulation signal increases during stochastic resonance at the expense of the "deterministic" noise energy which must decrease outside a small neighborhood of the frequency axis in order that the total energy be preserved.

Observe that the results of this work were calculated using the "two-state" dynamics method. Application of the complete dynamics method leads to the same qualitative results.

6. Conclusion

The results of our numerical investigation give convincing evidence of the realization of the stochastic resonance phenomenon in the driven Chua's circuit. Our numerical data confirms the conclusions of Ref.24 concerning the SR phenomenon in quasi-hyperbolic systems with chaotic dynamics. Unlike bistable systems with fixed point attractors, the interaction between chaotic attractors having a "chaos-chaos" type intermittency includes more possibilities. In particular, an increase in the SNR can take place by tuning the system parameters without external noise. In this case, the intrinsic chaotic dynamics plays the role of "deterministic" noise.

From a statistical perspective, chaotic bistable systems have two characteristic time constants (or two characteristic frequencies). One of them is related to the random process of transitions and is determined by the probability density function of the residence time of the trajectory in each interacting attractor. The second characteristic time constantis related to the intrinsic chaotic

dynamics of the interacting attractors. The external harmonic excitation result in the appearance of a third characteristic time constant in the system; namely, a deterministic modulation period T_0.

In chaotic systems, the SR-phenomenon can take place via a coherent interaction between the statistical process of transitions and the deterministic periodic modulation. At the resonant frequency, the structure of the residence time probability density is characterized by the presence of a series of peaks (maxima) near the discrete values $\tau^m=m/2$ (m=1,3,5,...). Hence, at the moment of stochastic resonance the system exhibits the most probable switching frequencies $\omega_s^m=2\omega_0/m$, m=1,3,5,.... Optimal conditions of SR are reached when the mean switching frequency is equal to twice the modulation frequency (m=1). Note that the properties of the SR-phenomenon caused by the interaction between frequencies ω_s^m and ω_0 are similar qualitatively to those predicted in the classical theory of SR[1-7].

The birth of a stable limit cycle following the application of an external modulation is a typical phenomenon in quasi-hyperbolic systems[14,16,21]. In this case, the classical resonance phenomenon takes place, when the amplitude of the periodic modulation increases very strongly at some rational ratio of frequencies. The addition of an external noise in this case reduces the amplitude of the modulation signal and, therefore, suppresses the effect of the classical resonance. A further increase in the noise intensity leads to a continuous transition from the classical resonance phenomenon to a stochastic one (SR).

The results of this work combined with the data from Ref.[24], testify convincingly that the stochastic resonance effects are quite general. The properties established in this paper are a consequence of some fundamental laws of nonlinear oscillations. The necessary condition for stochastic resonance to occur is an interaction of attractors. This process can be induced by an external noise. In this

case, the same classical SR-phenomenon takes place. Moreover, the switching process can be induced strictly by the dynamical properties of the system (the dynamical intermittency). In this case, we have the possibility to realize the SR-phenomenon in the dynamical system without any external noise excitation. One natural generalization is to investigate the SR-phenomenon by tuning the system parameter in the presence of a fixed intensity noise.

In closing, we remark that the results of this work represent only the beginning of a more comprehensive investigation of the SR-phenomenon in chaotic systems. We hope that further investigations will allow us to obtain new scientific results having some practical applications.

Acknowledgement

The authors would like to thank Prof. Frank Moss and Dr. Lutz Shimansky-Geier for attracting our attention to the fascinating phenomenon of stochastic resonance.

References

1. R.Benzi, A.Sutera, A.Vulpiani. "The mechanism of stochastic resonance", *J.Phys.A* **14** (1981), L453-L457.

2. S.Fauve, F.Heslot."Stochastic resonance in a bistable system", *Phys.Lett.A* **97** (1983), 5-8.

3. B.McNamara, K.Wiesenfeld, R.Roy. "Observation of stochastic resonance in a ring laser", *Phys. Rev. Lett.*,60 (1988),2625-2629.

4. B.McNamara, K.Wiesenfeld. "Theory of stochastic resonance", *Phys.Rev.A* **39** (1989), 4854-4869.

5. P.Jung, P.Hanggi. "Stochastic nonlinear dynamics modulated by external periodic forces", *Europhys. Lett.* **8** (1989), 505-511.

6. C.Presila, F.Marchesoni, L.Gammaitoni, "Periodically time-modulated bistable systems: nonstationary statistical properties", *Phys.Rev.A* **40** (1989), 2105-2113.

7. P.Jung, P.Hanggi, "Resonantly driven Brownian motions: basic conceptions and exact results", *Phys.Rev.A* **41** (1990), 2977-2988. 8. L.Gammaitoni, F.Marchesoni, E.Menichella-Saetta, S.Santucci. "Stochastic resonance in bistable systems", *Phys.Rev.Lett.*, **62** (1989) 349-352.

9. L.Gammaitoni, E.Menichella-Saetta, S.Santucci., F.Marchesoni, C.Fresilla. "Periodically modulated bistable systems: stochastic resonance", *Phys.Rev.A* **40** (1989), 2114-2119.

10. T.Zhou, F.Moss, P.Jung. "Escape-time distributions of a periodically modulated bistable system with noise", *Phys.Rev.A* **42** (1990), 3161-3169.

11. F.Moss. "Stochastic resonance", *Rate processes in dissipative systems: 50 Years after Kramers*, edited by P.Hanggi and J.Troe, Ber. Bunsenges. Phys. Chem, 1991.

12. F.Moss. *Stochastic Resonance: From the Ice Ages to the Monkey's Ear*, Dept. of Physics of University of Missouri at Saint Louis, St. Louis, MO 63121, USA, January 1992.

13. H.A.Kramers. "Brownian motion in a field of force and the diffusion model of chemical reactions", *Physica*, **7** (1940), 284-
304.

14. V.S.Afraimovich and L.P.Shilnikov, "Strange attractors and quasi-attractors" in *Dynamics and Turbulence*, Pitman, NY, 1983, p.1-51.

15. W.Horsthemke, R.Lefever. *Noise-induced transitions. Theory and applications in physics, chemistry and biology*, Springer-Verlag, Berlin, 1984.

16. V.S.Anishchenko. *Complicated oscillations in simple systems*, Nauka, Moscow, 1990.

17. V.S.Anishchenko, A.B.Neiman. "Structure and properties of chaos in presence of noise". *Nonlinear Dynamics of Structures*, ed. R.Z.Sagdeev et al., World Scientific, Singapore, 1991, pp.21-48.

18. V.S.Anishchenko, M.A.Safonova. "Bifurcations of attractors in presence of fluctuations", *Journal of technical physics*, **57** (1987) 1931-1943.

19. V.S.Anishchenko, A.B.Neiman. "Noise induced transition in Lorenz model", *Letters to journal of technical physics*, **17** (1990) 43-47.

20. F.T.Arecci, R.Badii, A.Politi. "Low-frequency phenomena in dynamical systems with many attractors", *Phys.Rev.A* **29** (1984), 1006-1009.

21. V.S.Anishchenko. *Dynamical chaos in physical systems. Experimental investigation of self-oscillating circuits*, Teubner-Texte, Leipzig, 1989.

22. V.S.Anishchenko. "Interaction of attractors. Intermittency of the chaos-chaos type", *Letters to journal of technical physics*, **10** (1984) 629-633.

23. V.S.Anishchenko, A.B.Neiman. "Increasing of correlations time under chaos-chaos intermittency", *Letters to journal of technical physics*, **13** (1987), 1063-1066.

24. V.S.Anishchenko, A.B.Neiman, M.A.Safonova. "Stochastic resonance in chaotic systems", the report in the conference *Stochastic resonance*, San Diego, March, 29 - April, 4, 1992 (submitted to Journal of Statistical Physics).

25. L.O.Chua, M.Komuro, T.Matsumoto. "The double scroll family", *IEEE Trans. in circuits and systems*, **33** (1986) 1073-1118.

Figure captions

Fig.1. The 2-parameter bifurcation diagram of the system (1) (drawn with m_0=-1/7, m_1=2/7, ε_0=0, D=0)[25] in the α-β plane.

Fig.2. Two-dimensional projections of the phase portraits of two symmetrical Rossler attractors of the autonomous system (1) at α=8.6, β=14.286

Fig.3. Transformation of the output signal $x(t)$ of the system (1) by the "two-state" dynamics method: (a,b) α=8.6, β=14.286, ε_0=0.0, D=0.05; (c,d) α=8.9, β=14.286, ε_0=0.0, D=0.0.

Fig.4. The power spectrum of the chaotic process $x(t)$ of the system (1) for α=8.9, β=14.286, ε_0=0.1, ω_0=0.6, D=0.0: (a) calculated by the complete dynamics method, (b) calculated by the "two-state" dynamics method.

Fig.5. The residence time probability density function $p(\tau)$, (a); the power spectrum $S(\omega)$, (b); and the probability density function $p(x)$, (c), for α=8.6, β=14.286, ε_0=0.0, D=0.03. Here $\tau=t/T_0$, $T_0=2\pi/0.6$.

Fig.6. The residence time probability density function $p(\tau)$, (a); the power spectrum $S(\omega)$, (b); and the probability density function $p(x)$, (c), for α=8.9, β=14.286, ε_0=0.0, D=0.0. Here $\tau=t/T_0$, $T_0=2\pi/0.6$.

Fig.7. The phase portrait, (a), and the power spectrum, (b), of the Rossler attractor in the system (1) for α=8.6, β=14.286, D=0.0, ε_0=0.0.

Fig.8. The phase portrait, (a); and the power spectrum, (b); of the DSA in the system (1) for α=8.81, β=14.286, D=0.0, ε_0=0.0.

Fig.9. The probability density function $p(x)$, (a); and the power spectrum $S(\omega)$, (b); in the presence of a modulation signal ε_0=0.1, ω_0=0.6 at α=8.6, β=14.286, D=0.0.

Fig.10. The residence time probability density function $p(\tau)$ for different values of the modulation frequency: (a) ω_0=0.4, (b) ω_0=0.6, (c) ω_0=0.8. Here $\tau=t/T_0$, $T_0=2\pi/\omega_0$,

D=0.

Fig.11. Plots of the mean switching frequency ω_s: (a) ω_s versus the noise intensity D at α=8.6, β=14.286; (b) ω_s versus α at D=0.0, β=14.286; (c) ω_s versus β at D=0.0, α=8.6 in the presence of modulation ε_0=0.1, ω_0=0.6.

Fig.12. The signal-to-noise ratio versus the parameter α for different values of the noise intensity D at ε_0=0.1, ω_0=0.6, β=14.286.

Fig.13. The residence time probability density function $p(\tau)$ in the presence of both noise and modulation signal with amplitude ε_0=0.1 and the frequency ω_0=0.6: (a) α=8.75, β=14.286, (b) α=8.775, β=14.286.

Fig.14. The signal-to-noise ratio versus the parameter β at α=8.6, ω_0=0.6, ε_0=0.1, D=0.0.

Fig.15. The plot of SNR(D) corresponding to α=8.6, β=14.286, ω_0=0.6, ε_0=0.1.

Fig.16. The plots of SNR(α) (a), $p(\tau)$ (b) and $S(\omega)$ (c) in the absence of noise (D=0.0) at ω_0=0.35, ε_0=0.15, β=14.286.

Fig.17. The plots of SNR(α) (a), $p(\tau)$ (b) and $S(\omega)$ (c) in the presence of noise (D=5*10^{-3}) at ω_0=0.35, ε_0=0.15, β=14.286.

Fig.18. The plot of SNR(D) corresponding to α=8.6, β=14.286 in the presence of a modulation signal with frequency ω_0=0.35 and amplitude ε_0=0.15.

Fig.19. The plot of SNR(α) (a), the phase portrait of the phase-locked limit cycle (b) and the power spectrum (c) of this stable limit cycle at β=5.0, D=0.0 in the presence of a modulation signal with ω_0=0.25, ε_0=0.07. The limit cycle and its power spectrum are drawn for α=4.1.

Fig.20. Dependencies of the SNR(α) on α for different values of the noise intensity D at β=5.0, ω_0=0.25, ε_0=0.07.

Fig.21. Power spectra of the chaotic process $w(t)$ at the precise parameter for SR (α=8.875, β=14.286, D=0.005) in the absence of a modulation signal (the dashed curve)

and with the modulation signal ε_0=0.15, ω_0=0.35.

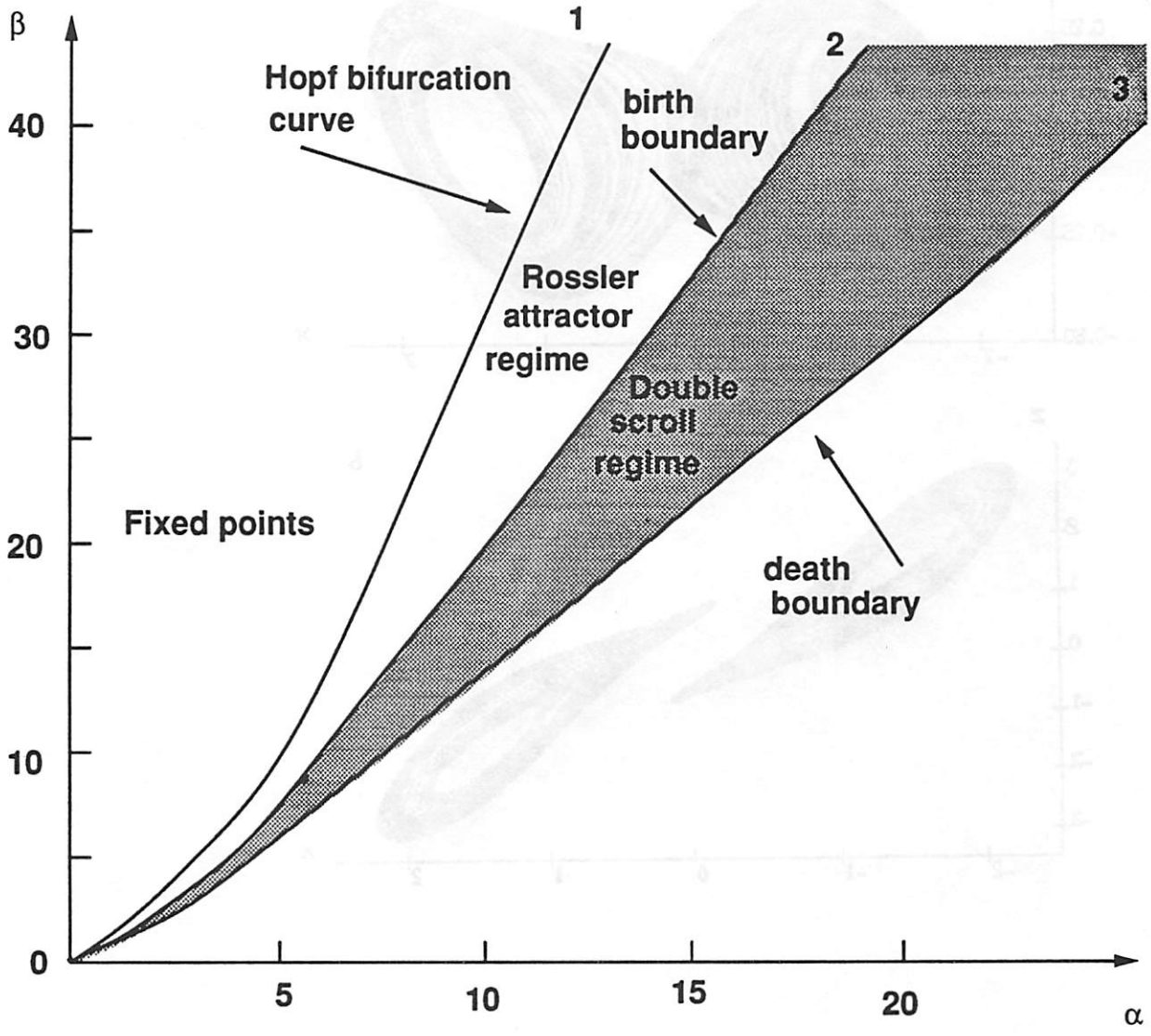
β
40
30
20
10
0
1
2
3
Hopf bifurcation curve
birth boundary
Rossler attractor regime
Double scroll regime
Fixed points
death boundary
5
10
15
20
α

Fig.1

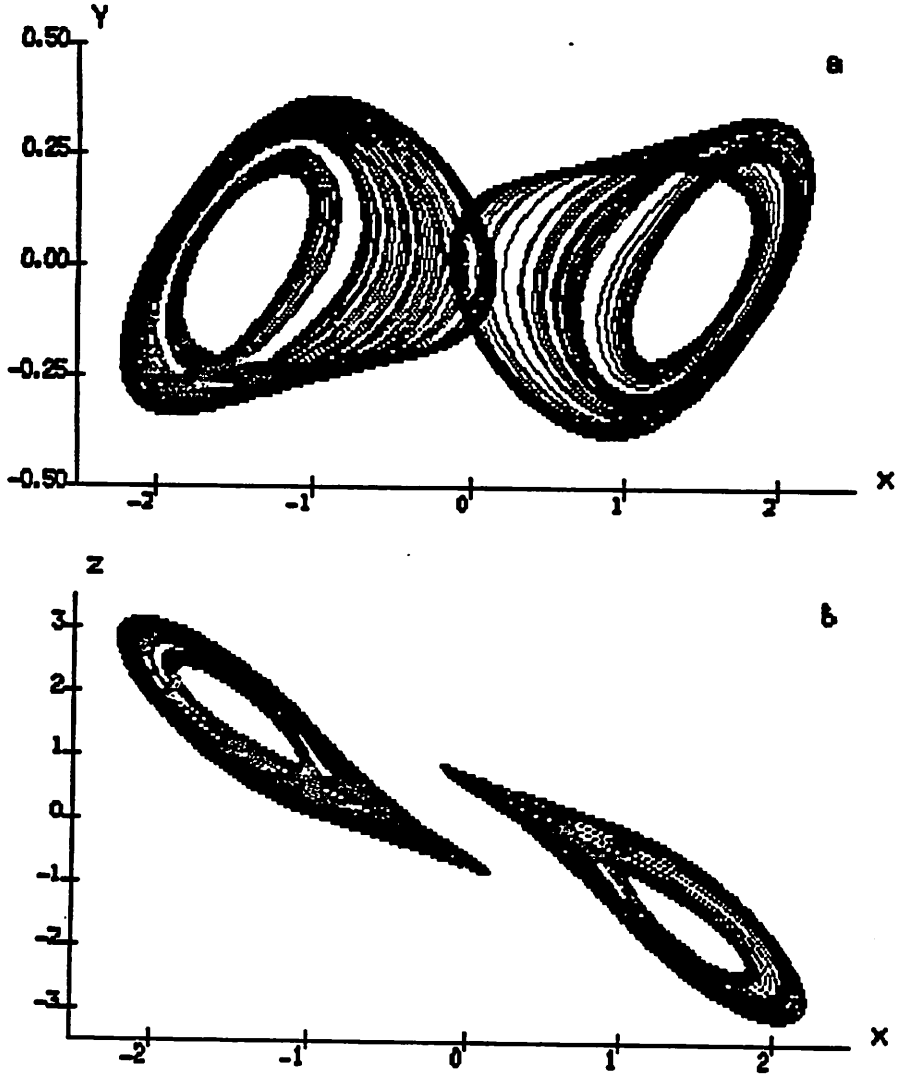

Fig.2

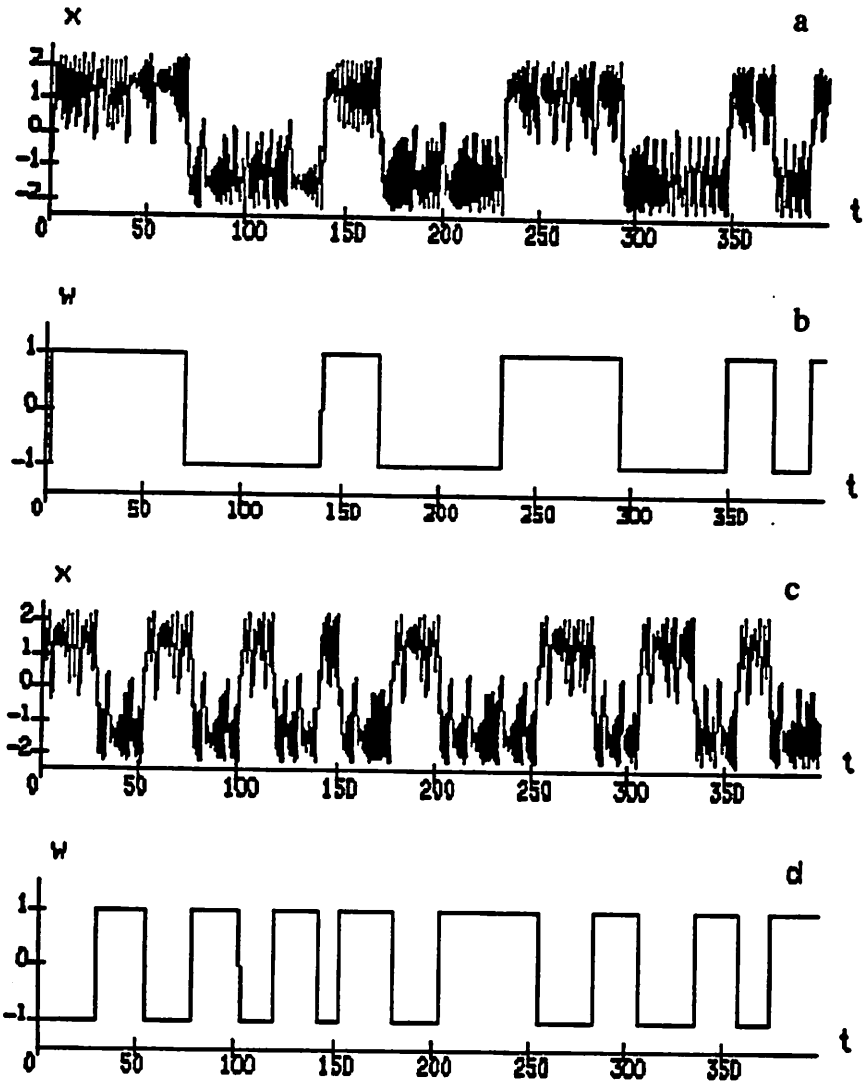
x
a
2
1
0
-1
-2
0
50
100
150
200
250
300
350
t
w
b
1
0
-1
0
50
100
150
200
250
300
350
t
x
c
2
1
0
-1
-2
0
50
100
150
200
250
300
350
t
w
d
1
0
-1
0
50
100
150
200
250
300
350
t

Fig. 3

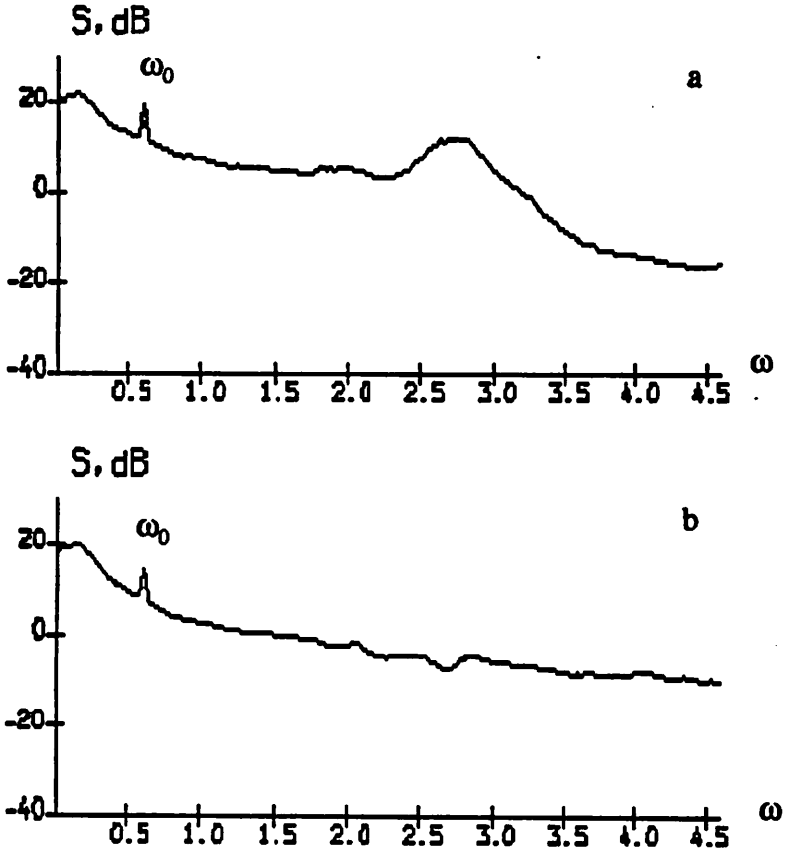
S, dB
ω_0
a
20
0
-20
-40
0.5
1.0
1.5
2.0
2.5
3.0
3.5
4.0
4.5
ω
S, dB
ω_0
b
20
0
-20
-40
0.5
1.0
1.5
2.0
2.5
3.0
3.5
4.0
4.5
ω

Fig. 4

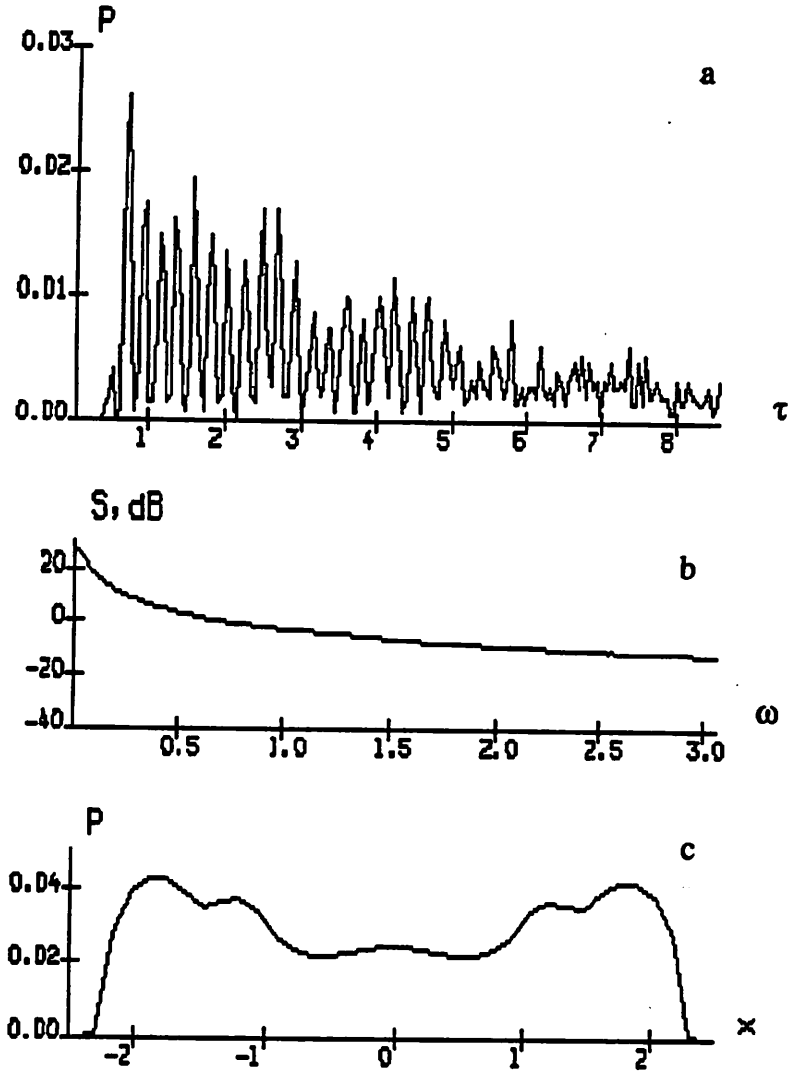
P
0.03
0.02
0.01
0.00
1
2
3
4
5
6
7
8
τ
a
S, dB
20
0
-20
-40
0.5
1.0
1.5
2.0
2.5
3.0
ω
b
P
0.04
0.02
0.00
-2
-1
0
1
2
x
c

Fig.5

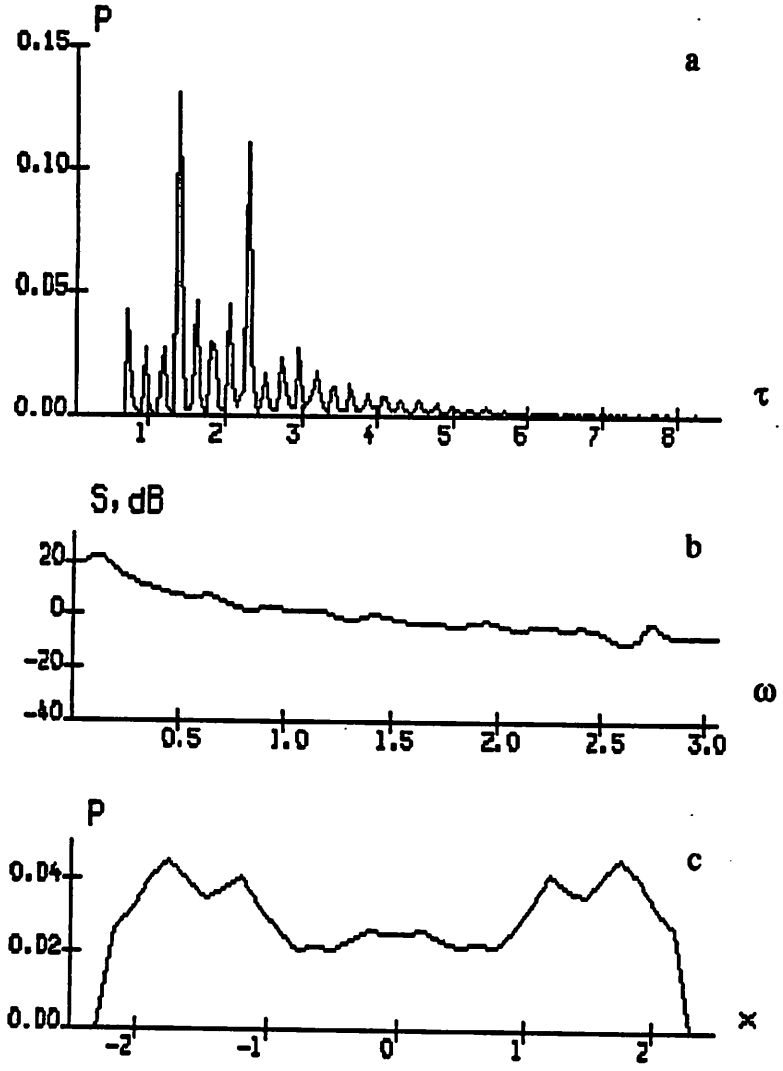
P
0.15
0.10
0.05
0.00
1
2
3
4
5
6
7
8
a
τ
S, dB
20
0
-20
-40
0.5
1.0
1.5
2.0
2.5
3.0
b
ω
P
0.04
0.02
0.00
-2
-1
0
1
2
c
x

Fig. 6

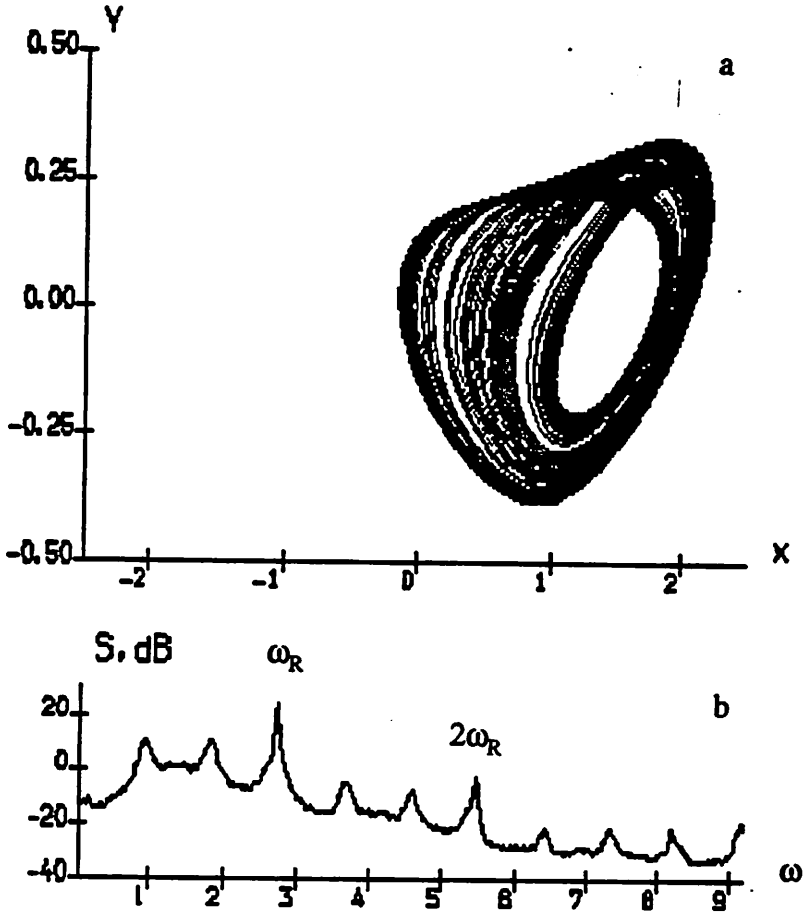
Y
0.50
0.25
0.00
-0.25
-0.50
a
X
-2
-1
0
1
2
S, dB
ω_R
$2\omega_R$
b
20
0
-20
-40
1
2
3
4
5
6
7
8
9
ω

Fig. 7

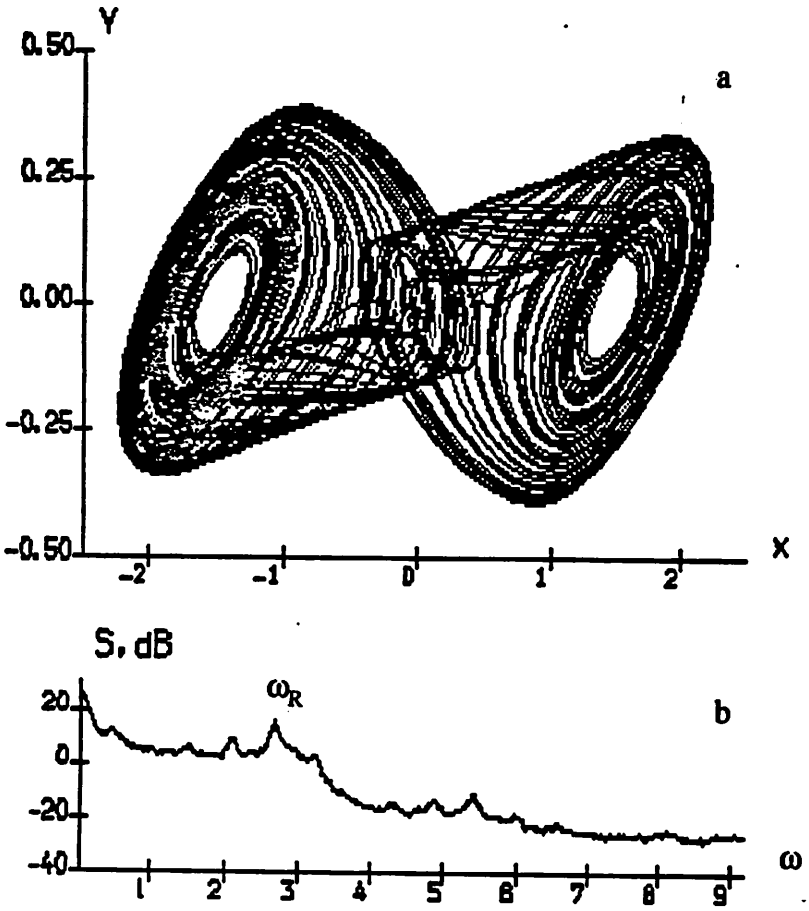
Y
0.50
0.25
0.00
-0.25
-0.50
-2
-1
0
1
2
X
a
S, dB
20
0
-20
-40
ω_R
1
2
3
4
5
6
7
8
9
ω
b

Fig 8

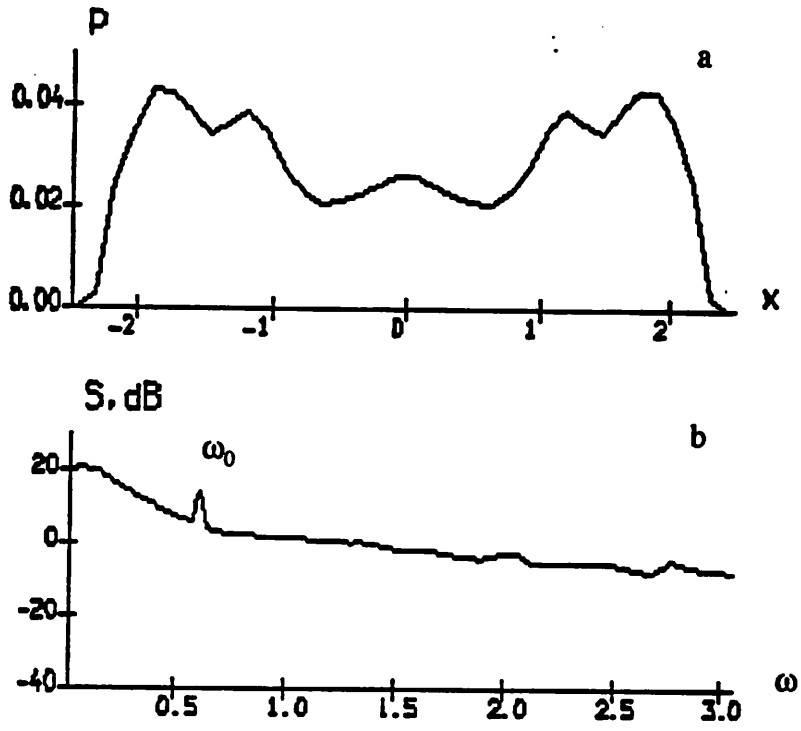

Fig. 9

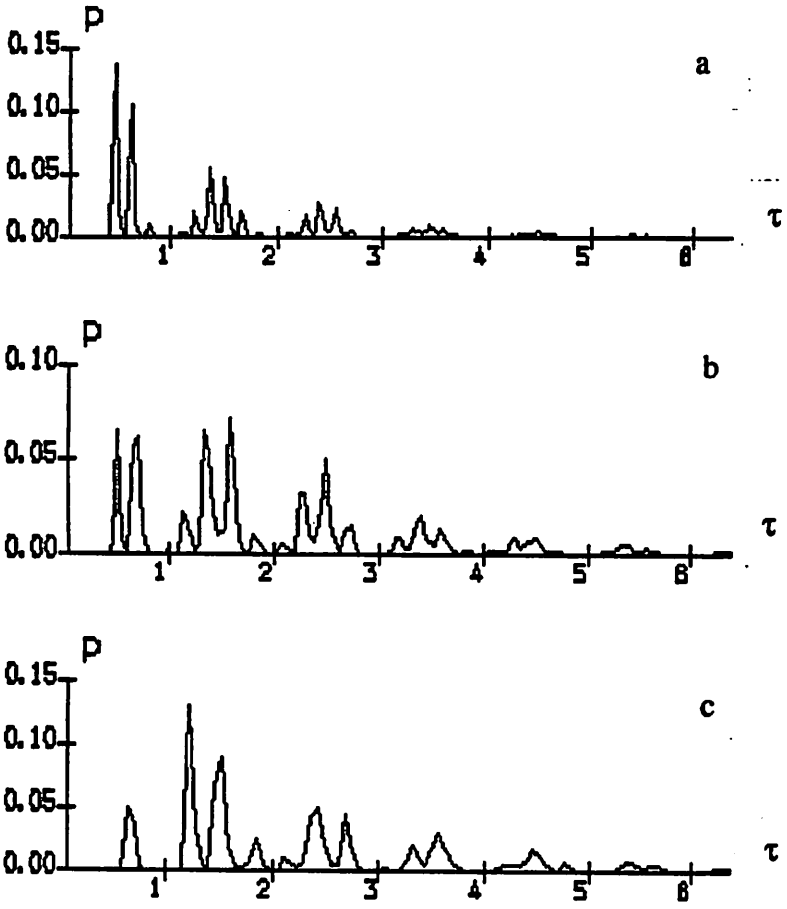
P
0.15
0.10
0.05
0.00
a
τ
1
2
3
4
5
6
P
0.10
0.05
0.00
b
τ
1
2
3
4
5
6
P
0.15
0.10
0.05
0.00
c
τ
1
2
3
4
5
6

Fig.10

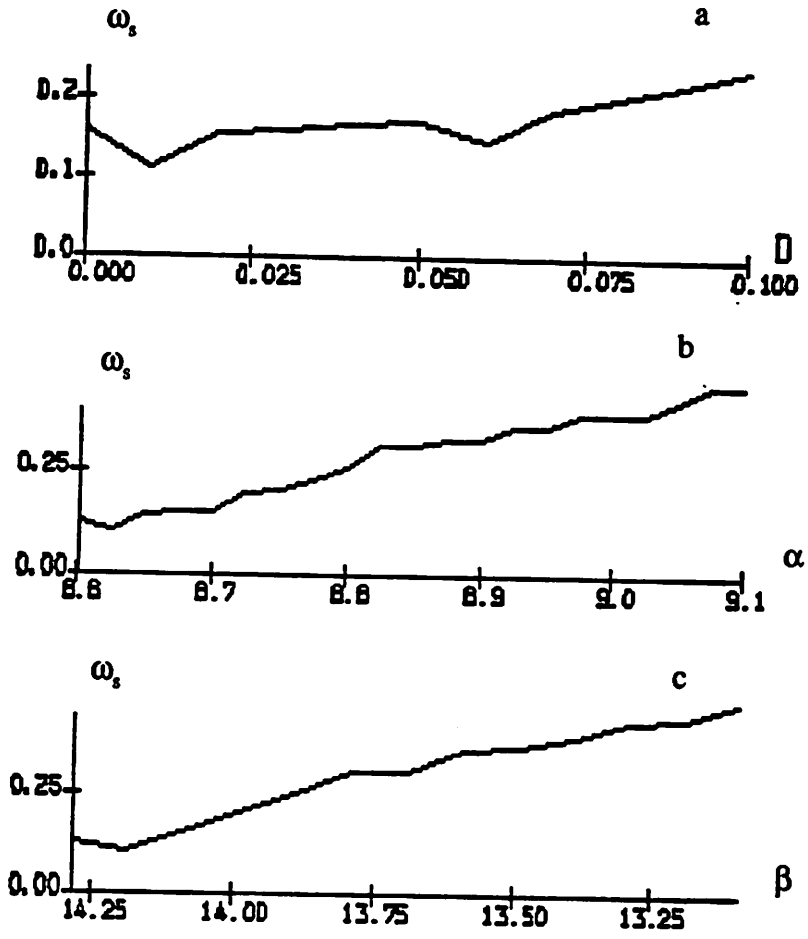
ω_s
a
0.2
0.1
0.0
0.000
0.025
0.050
0.075
0.100
D
ω_s
b
0.25
0.00
8.6
8.7
8.8
8.9
9.0
9.1
α
ω_s
c
0.25
0.00
14.25
14.00
13.75
13.50
13.25
β

Fig. 11

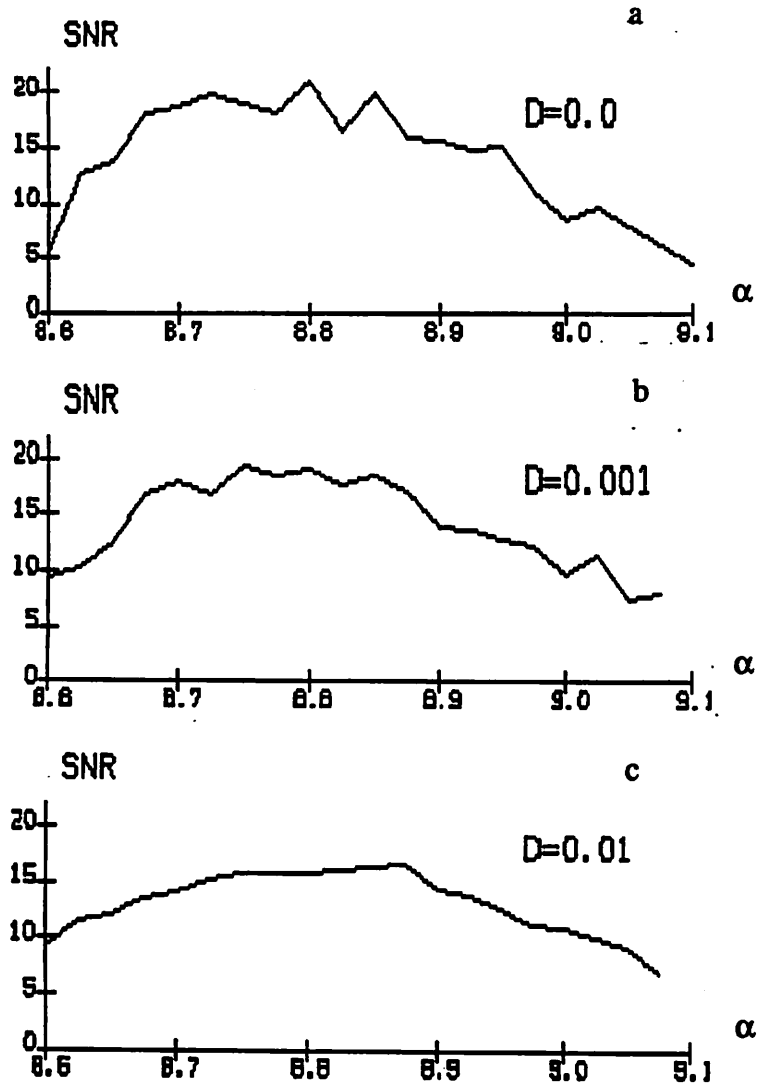
a
SNR
D=0.0
20
15
10
5
0
8.6
8.7
8.8
8.9
9.0
9.1
α
b
SNR
D=0.001
20
15
10
5
0
8.6
8.7
8.8
8.9
9.0
9.1
α
c
SNR
D=0.01
20
15
10
5
0
8.6
8.7
8.8
8.9
9.0
9.1
α

Fig.12

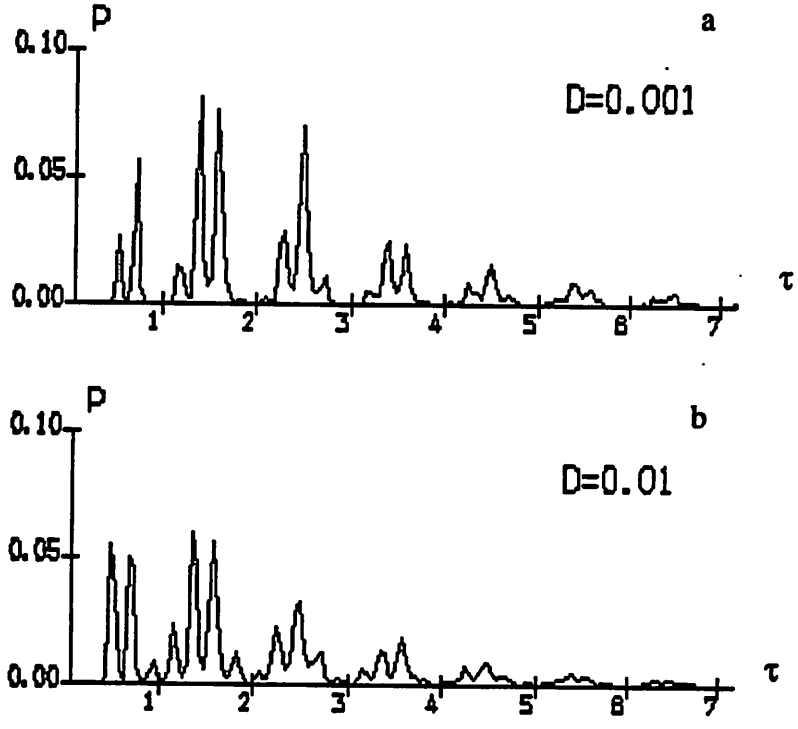

Fig. 13

Fig. 14

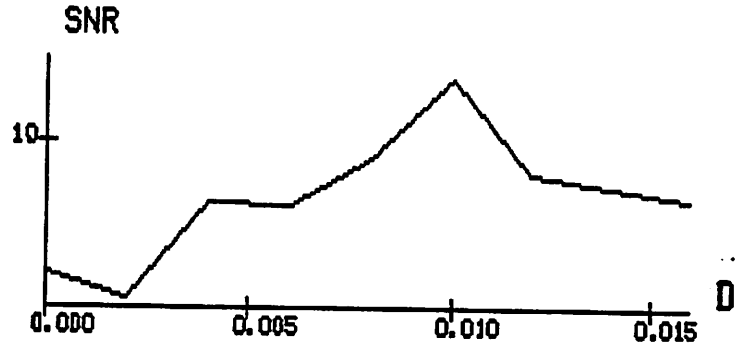

Fig. 15

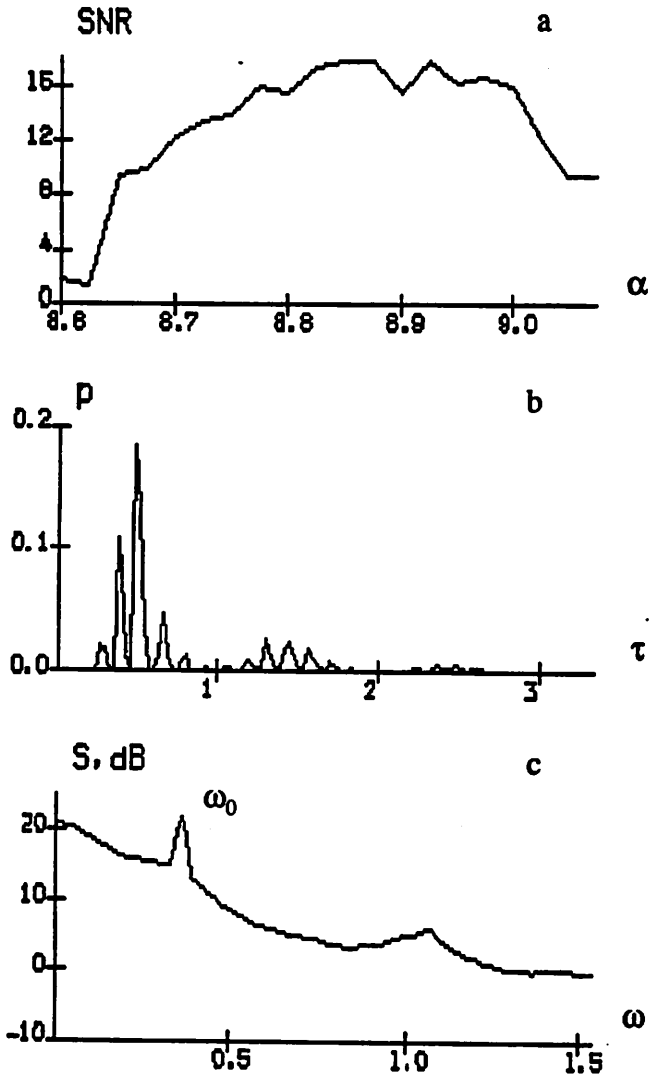
SNR
a
16
12
8
4
0
8.6
8.7
8.8
8.9
9.0
α
p
b
0.2
0.1
0.0
1
2
3
τ
S, dB
c
ω0
20
10
0
-10
0.5
1.0
1.5
ω

Fig. 16

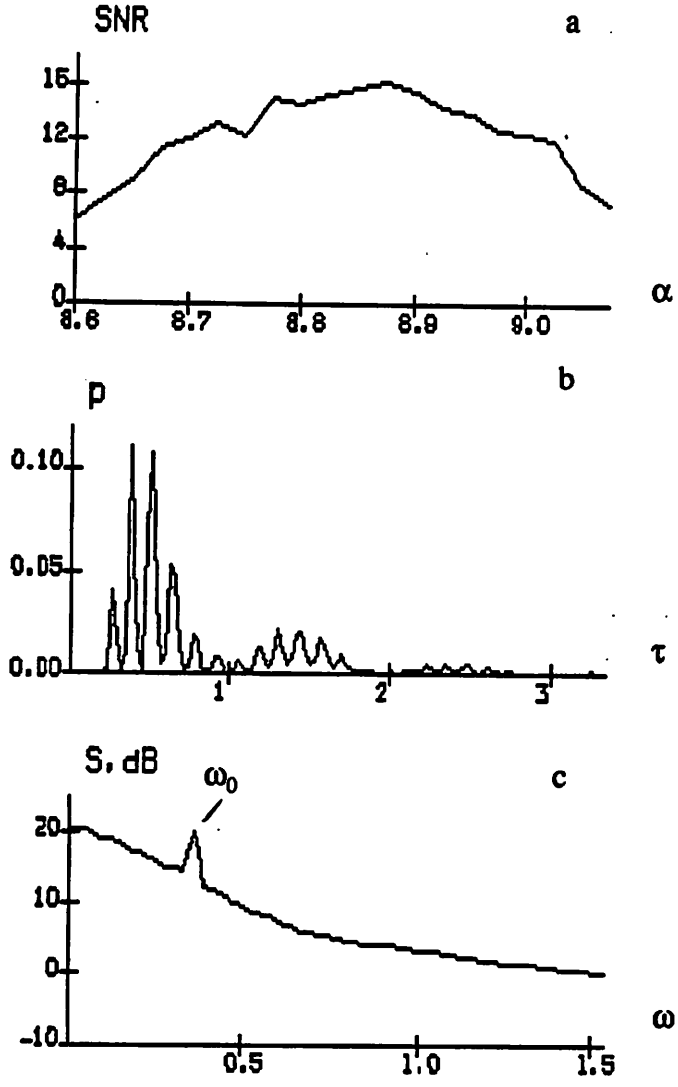
SNR
a
16
12
8
4
0
8.6
8.7
8.8
8.9
9.0
α
p
b
0.10
0.05
0.00
1
2
3
τ
S, dB
ω0
c
20
10
0
-10
0.5
1.0
1.5
ω

Fig. 17

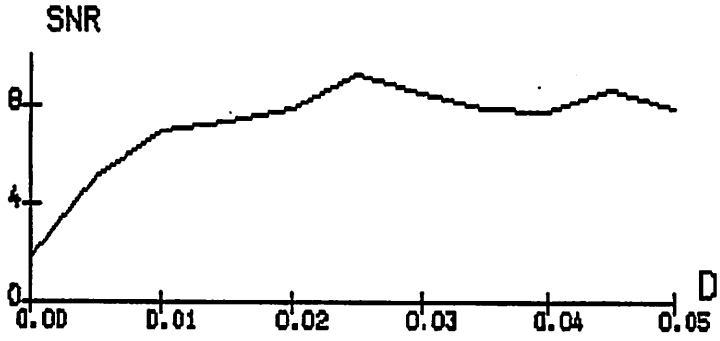

Fig. 18
Pue 18

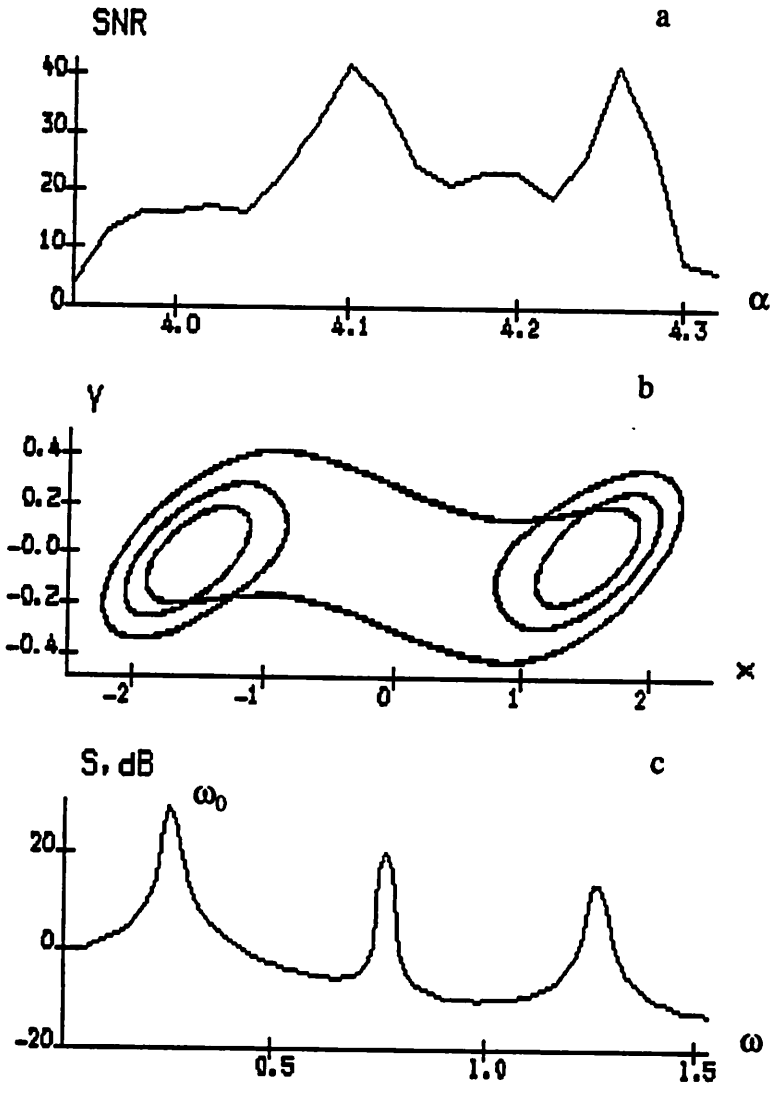
SNR
a
40
30
20
10
0
4.0
4.1
4.2
4.3
α
Y
b
0.4
0.2
-0.0
-0.2
-0.4
-2
-1
0
1
2
x
S, dB
c
ω0
20
0
-20
0.5
1.0
1.5
ω

Fig 19

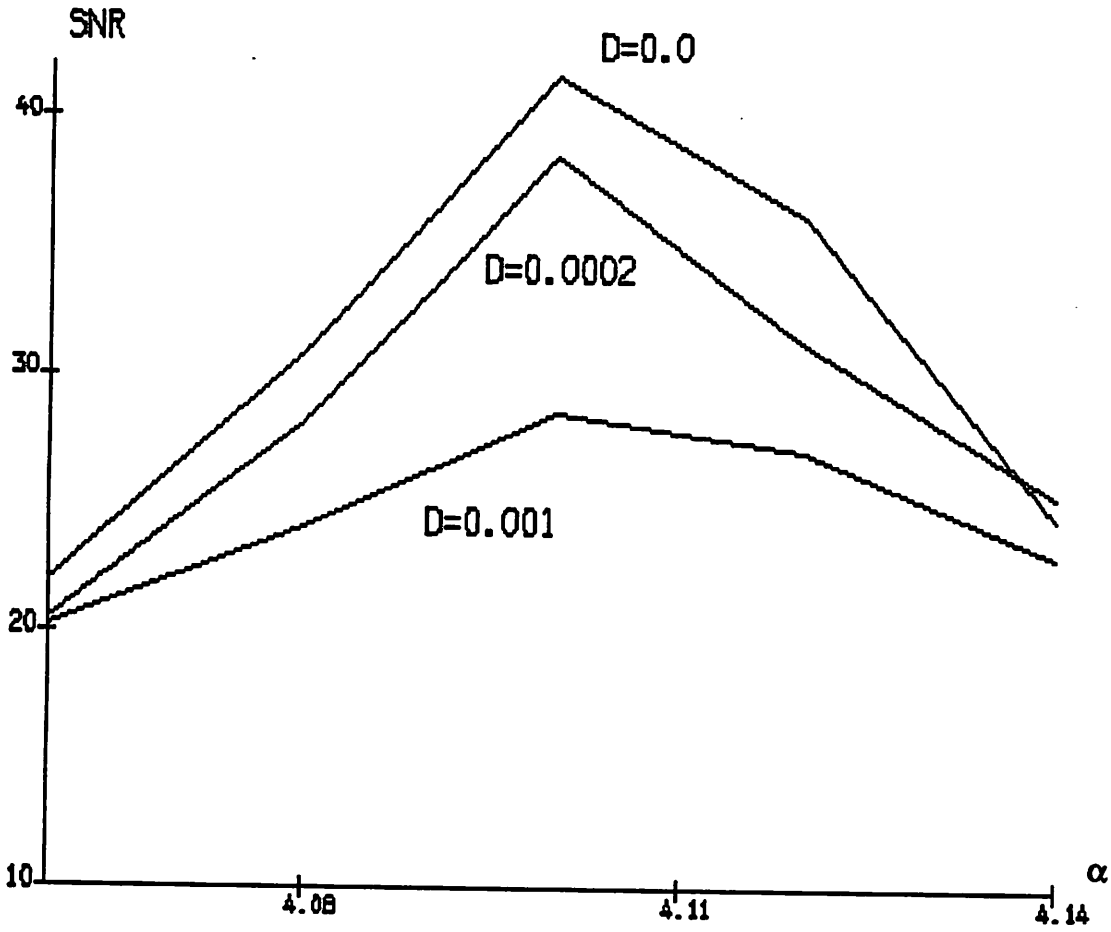

Fig. 20

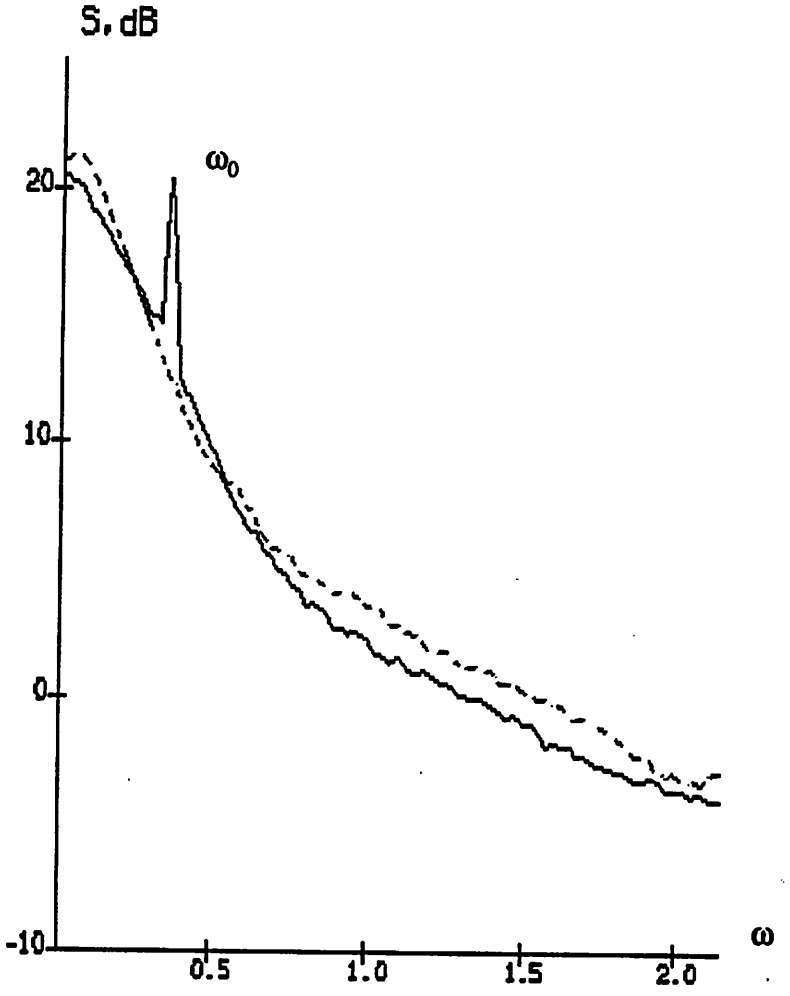

Fig. 21